Biosensors and Bioelectronics 62 (2014) 73–78

Contents lists available at ScienceDirect

Biosensors and Bioelectronics

journal homepage: www.elsevier.com/locate/bios

Facile synthesis of β-lactoglobulin-functionalized multi-wall carbon nanotubes and gold nanoparticles on glassy carbon electrode for electrochemical sensing

Xin Du [a], Zhiying Miao [a], Di Zhang [a], Yuxin Fang [b], Min Ma [a], Qiang Chen [a,*]

[a] The Key Laboratory of Bioactive Materials, Ministry of Education, College of Life Science, Nankai University, Weijin Road No. 94, Tianjin 300071, PR China
[b] College of Acumox and Tuina, Tianjin University of Traditional Chinese Medicine, Tianjin 300193, PR China

ARTICLE INFO

Article history:
Received 9 May 2014
Received in revised form
3 June 2014
Accepted 12 June 2014
Available online 20 June 2014

Keywords:
β-Lactoglobulin
Multi-wall carbon nanotube
Gold nanoparticles
Nanocomposite
Biosensor

ABSTRACT

A facile approach was developed for the preparation of nanocomposite based on β-lactoglobulin (BLG)-functionalized multi-wall carbon nanotubes (MWCNTs) and gold nanoparticles (GNPs) for the first time. Owing to the amphipathic nature, BLG can be adopted onto the surface of MWCNTs to form BLG-MWCNTs with uniform dispersion in water. Taking advantage of sulfhydryl groups on BLG-MWCNTs, GNPs were decorated on the BLG-MWCNTs-modified glassy carbon electrode (GCE) by electrodeposition. The nanocomposite was characterized by transmission electron microscopy, scanning electron microscopy and X-ray spectroscopy analysis. Cyclic voltammetry and chronoamperometric method were used to evaluate the electrocatalytic ability of the nanocomposite. Furthermore, a glucose biosensor was developed based on the immobilization of glucose oxidase with cross-linking in the matrix of bovine serum albumin (BSA) on the nanocomposite modified GCE. The resulting biosensor exhibited high sensitivity (3.98 μA mM^{-1}), wider linear range (0.025–5.5 mM), low detection limit (1.1 μM at the signal-to-noise ratio of 3) and fast response time (within 7 s) for glucose detection.

1. Introduction

Carbon nanotubes (CNTs), composed of well-ordered cylinders of sp^2-hybridized carbon atoms, have attracted an increasing attention in recent years. These nanomaterials can be classified as single-walled carbon nanotubes and multi-walled carbon nanotubes (MWCNTs). Each of MWCNTs shares a common longitudinal axis and contains several concentric tubes. Due to their excellent electrical conductivity, high stability, large surface area and mechanical stability, CNTs provided potential application in various fields (Atthipalli et al., 2011; Elouarzaki et al., 2014). However, CNTs have a tendency to aggregate in most solvents and form tangled network structures, the efficient and large scale application of CNTs is difficult (Chen et al., 1998). To overcome these limits, many efforts have been devoted to modify the surface of CNTs through covalent (Geyik et al., 2014; Shao et al., 2011) and non-covalent (Majeed et al., 2012) methods. Unfortunately, drastic and complex covalent modification of MWCNTs usually perturbs the interior structure of CNTs (Voge et al., 2013), and thus deteriorates their physical and chemical properties. The non-covalent methods are based on physisorption of dispersants molecules to the surface of CNTs. It is difficult for most of them to be applied to living systems, although there are numerous dispersants for CNTs, such as diallyldimethylammonium chloride (S.Y. Wang et al., 2011) and lauryl sodium sulfate (Zhang et al., 2014). Therefore, it is valuable and important to find a facile approach to fabricating functionalized CNTs which have favorable dispersibility and biocompatibility. Consequently, proteins are employed for dispersing CNTs because of their non-toxic and biocompatible nature (Munoz et al., 2013; Wang et al., 2010).

β-Lactoglobulin (BLG), a small globular protein present in the milk of several mammals, has 162 amino acid residues with different hydrophilicity (Liang et al., 2008; Mensi et al., 2013). Due to the amphiphilic property, BLG can adhere to a solid surface, and thus improve the dispersibility of hydrophobic particles in water. The experimental works and molecular simulations have been reported (Fragneto et al., 2000; Sahihi et al., 2013). Moreover, BLG has been reported to be an effective dispersant for C_{60} derivatives (Belgorodsky et al., 2007).

Nanocomposite has been widely utilized in biosensors in the last several years. Many works focused on decorating CNTs with metal nanoparticles due to their synergistic effect (Abdelhalim et al., 2014; Fang et al., 2012). GNPs have extraordinary catalytic property, good conductivity and biocompatibility, and thus they have found application in a range of electrochemical applications.

* Corresponding author. Tel.: +86 22 23507273; fax: +86 22 23506122.
E-mail address: qiangchen@nankai.edu.cn (Q. Chen).

http://dx.doi.org/10.1016/j.bios.2014.06.030
0956-5663/

BLG may be suitable for assembling gold nanoparticles because BLG contains sulfhydryl groups (Feng et al., 2009).

The aim of this work is to develop a facile approach to preparing a promising nanocomposite based on BLG-MWCNTs-GNPs. Initially, the MWCNTs were satisfactorily dispersed by using BLG with doubly distilled water. Then, the BLG-MWCNTs formed a uniform film on the surface of a glassy carbon electrode (GCE). Subsequently, GNPs were decorated on the BLG-MWCNTs modified GCE by electrodeposition. In order to reveal the catalysis activity of the modified GCE, we developed a glucose biosensor. To the best of our knowledge, this is the first demonstration of an electrochemical biosensor based on the integration of glucose oxidase (GOD) with BLG-MWCNTs-GNPs nanocomposite.

2. Experimental

2.1. Chemicals and reagents

MWCNTs (> 50 nm diameter, 10 μm average length and > 95% purity) were obtained from Alpha Nano Technology Co., Ltd. (China). β-Lactoglobulin, $HAuCl_4 \cdot 3H_2O$, GOD, BSA and L-cysteine were purchased from Sigma (USA). Glucose was obtained from Tianjin Damao Chemical Reagent Co. (China). Phosphate buffer solution (PBS, 0.1 M, pH 7.0) was prepared by Na_2HPO_4 and NaH_2PO_4. All aqueous solutions were prepared with doubly distilled water.

2.2. Measurements

Electrochemical measurements were performed in an electrochemical cell using a conventional 283 Potentiostat-Galvanostat electrochemical workstation (EG&G PARC with M270 software) at room temperature. A conventional three-electrode system involving the modified GCE as a working electrode, an Ag/AgCl (saturated KCl) as a reference electrode and a platinum wire (1 mm diameter) as a counter electrode, was employed for all electrochemical experiments. In steady-state amperometric experiment, the potential was set at +600 mV under gentle magnetic stirring. Transmission electron microscopy (TEM) images were collected on Tecnai G2 F20 instrument (Philips Holland) equipped with an energy-dispersive X-ray spectroscopy (EDX) analyzer. The surface morphology was recorded by using scanning electron microscopy (SEM, QUANTA 200, FEI Co.).

2.3. Dispersion of MWCNTs in BLG solutions

6 mg MWCNTs were dissolved in 3 mL BLG solution (2 mg/mL) with help of ultrasonic agitation for 90 min. The MWCNTs functionalized by BLG (BLG-MWCNTs) were obtained from the suspension by centrifugation at 4000 rpm for 15 min.

2.4. Fabrication of modified electrode

Unmodified GCE was polished with 0.3 and 0.05 μm alumina powders and then ultrasonically cleaned in double distilled water and ethanol for 10 min to remove the physically adsorbed substance. The prepared electrode was dried with nitrogen gas. Eight μL of BLG-MWCNTs suspension (2 mg/mL) was dropped onto the GCE surface to obtain BLG-MWCNTs/GCE. The BLG-MWCNTs/GCE was immersed in 20 mL deposition solution (5 mM $HAuCl_43H_2O_2$, 0.1 mM L-cysteine, 0.1 M H_2SO_4) and applied a constant potential at −400 mV for 360 s to obtain the BLG-MWCNTs-GNPs/GCE. Glucose biosensor was prepared by casting 8 μL of the composite solution containing 125 μL GOD (5 mg/mL), 25 μL BSA (10 mg/mL), and 20 μL glutaraldehyde (2%) solutions onto the surface of BLG-MWCNTs-GNPs/GCE electrode, denoted as GOD/BSA/BLG-MWCNTs-GNPs/GCE, then the modified electrode was dried and stored at 4 °C in a refrigerator. The whole process of the fabrication is illustrated in Scheme 1.

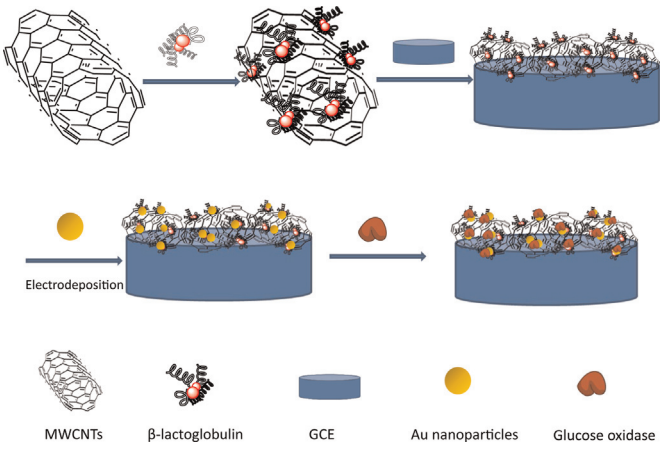

Scheme 1. A schematic illustration for the preparation of a glucose biosensor.

3. Results and discussion

3.1. Morphology

Because the MWCNTs tend to aggregate in aqueous solution, the dispersibility and stability of MWCNTs are critical factors in the following application. Owing to the amphiphilic properties, BLG has a high tendency to migrate to hydrophobic–hydrophilic interfaces and is able to encapsulate and dissolve hydrophobic molecules into aqueous media. Therefore, the BLG-MWCNTs suspension was stable for 30 days at room temperature as shown in Fig. S1B. On the contrary, the MWCNTs prepared without BLG aggregated at the bottom of the vials within 15 min (Fig. S1A).

The microstructures of the BLG-MWCNTs were examined by TEM and SEM under different magnifications. As shown in Fig. 1A and B, a core–shell structure of MWCNTs was clearly seen and the BLG-MWCNTs were much wider than the pristine MWCNTs, indicating the MWCNTs were wrapped by BLG with a thickness of about 7 nm. BLG contains two disulfide bonds and one free sulfhydryl group (Sakai et al., 2000). The surface of BLG-MWCNTs introduced abundant amino acid residues which may provide active sites to anchor nanoparticles. Fig. 1C and D demonstrates that the BLG-MWCNTs have been decorated with GNPs by electrodeposition. The lattice structure of GNPs was observed clearly under the high magnification. The surface microstructure of electrode has a significant influence on the performance and reactivity. Fig. 1E shows that a highly uniform BLG-MWCNTs film was established on the surface of GCE without tangled ropes, which suggests that BLG is an excellent dispersant for MWCNTs again. In order to confirm that the sample contains the elements of C and Au, the EDX analysis was done (Fig. 1F). The peaks of O and Cu in the spectrum should be from the substrate.

3.2. Electrocatalytic activity of BLG-MWCNTs-GNPs/GCE

Cyclic voltammetry (CV) of unmodified GCE (a), BLG-MWCNTs/GCE (b) and BLG-MWCNTs-GNPs/GCE (c) were conducted in 0.1 M KCl solution containing 10 mM $[Fe(CN)^6]^{3-}$ ions as shown in Fig. 2. For the BLG-MWCNTs-GNPs/GCE, a couple of well-defined peaks were observed at +290 mV and +186 mV. The peak-to-peak separations (E_p) were 130 mV, 114 mV and 104 mV for unmodified

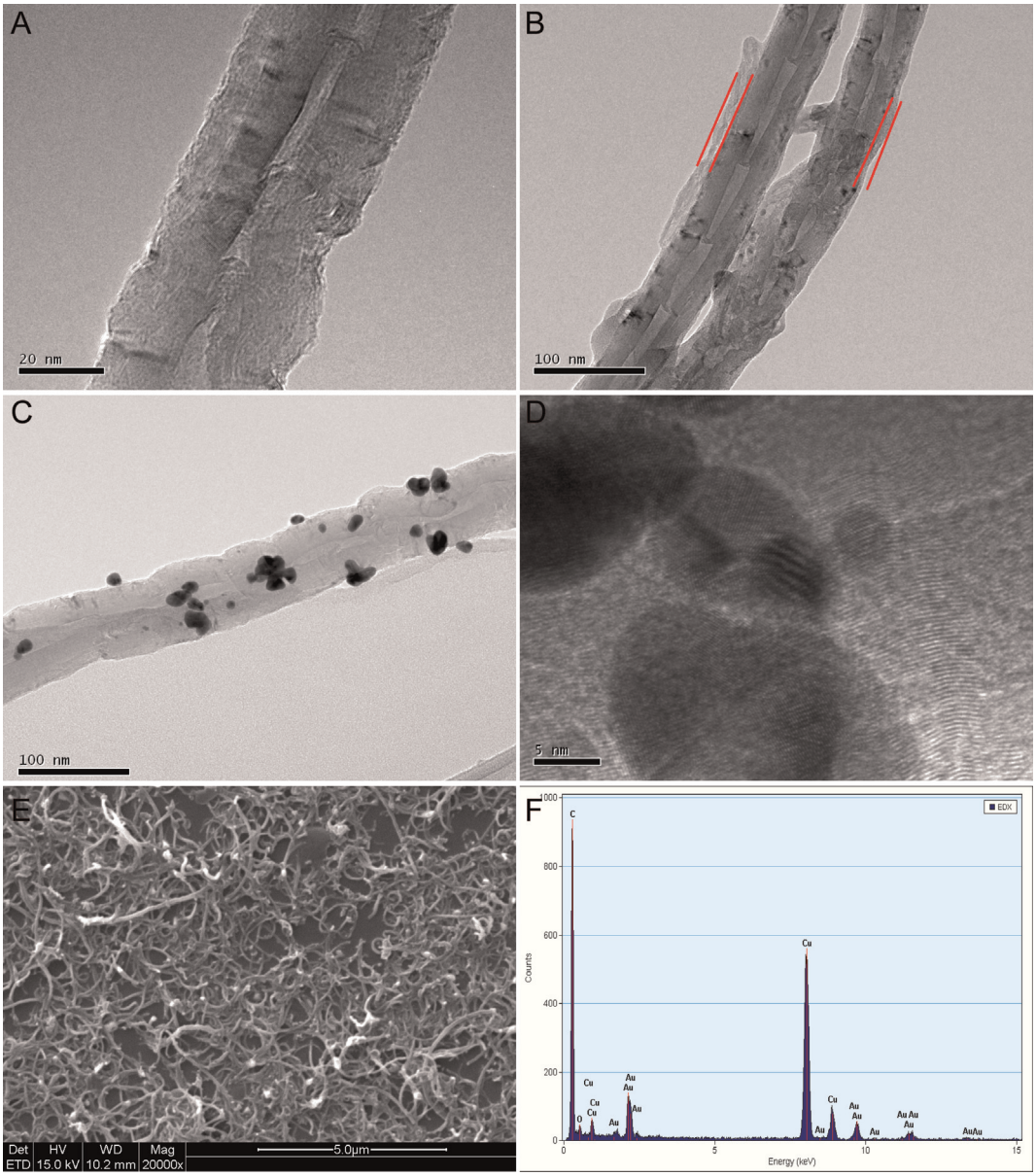

Fig. 1. TEM images of (A) pristine MWCNTs and (B) BLG-MWCNTs; TEM images of BLG-MWCNTs-GNPs under different magnification (C and D); (E) SEM images of BLG-MWCNTs; (F) EDX analysis of BLG-MWCNTs-GNPs.

GCE BLG-MWCNTs/GCE and BLG-MWCNTs-GNPs/GCE, respectively, which indicated the fast electron-transfer kinetics of BLG-MWCNTs-GNPs/GCE. The microscopic electroactive areas of modified electrodes can be estimated according to the Randles–Sevcik equation (Gao et al., 2006)

$$I_p = 2.69 \times 10^5 A D^{1/2} n^{3/2} \gamma^{1/2} C \quad (1)$$

where A corresponds to the electroactive surface area of electrode (cm^2), D represents the diffusion coefficient of the molecule in solution which is $(6.70 \pm 0.02) \times 10^{-6}$ cm^2 s^{-1}, n is the number of electron participating in the reaction which is equal to 1, γ is the scan rate ($V\ s^{-1}$), C is the concentration of the probe molecule in the solution which is 10 mM and I_p relates to the redox peak current. According to the above equation, we can calculate the value of electroactive surface area for BLG-MWCT-GNPs/GCE to be 0.08 cm^2, which is 2.08- and 1.25-times higher than those of unmodified GCE and BLG-MWCNTs/GCE, respectively. These results revealed that the BLG-MWCNTs-GNPs film is more suitable to facilitate electron transfer between $[Fe(CN)^6]^{3-}$ and the working electrode. This may result from the combined effects of MWCNTs (large edge plane/basal plane ratio, enhanced conductivity and rapid electrode kinetics) and GNPs (good catalytic activity and large surface area).

Fig. 3 shows CVs of unmodified GCE (a), GNPs/GCE (b), BLG-MWCNTs/GCE (c) and BLG-MWCNTs-GNPs/GCE (d) in 0.5 M H_2SO_4. We can see that the BLG-MWCNTs/GCE has a higher charging current than unmodified GCE due to the increase of the electrode surface area and electroconductibility. For the GNPs/GCE and BLG-MWCNTs-GNPs/GCE, an increased anodic current was observed around 1.3 V, which can be assigned to the oxidation of GNPs. The peak at around 0.9 V is due to the reduction of the oxide on the GNPs (Haghighi et al., 2011). The reaction of GNPs can be described by the following equation (Burke et al., 1994):

$$2Au + 3H_2O \rightarrow Au_2O_3 + 6H^+ + 6e^- \quad (2)$$

The redox peak current of BLG-MWCNTs-GNPs/GCE was approximately 3.8-times higher than that of GNPs/GCE, probably due to synergistic effects of BLG-MWCNTs and GNPs. Furthermore,

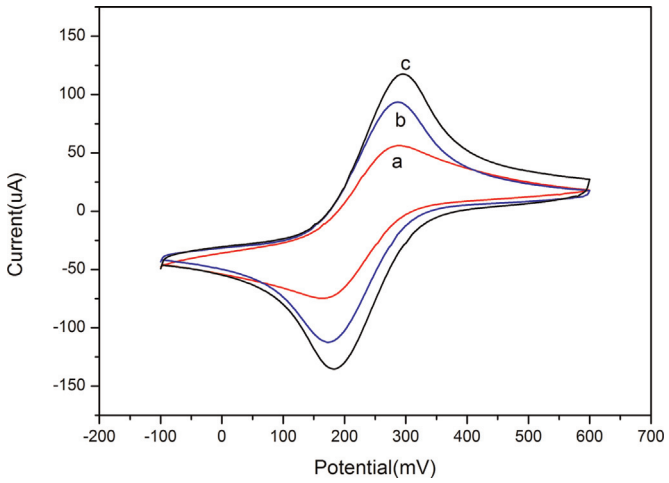

Fig. 2. Cyclic voltammograms of (a) unmodified GCE, (b) BLG-MWCNTs/GCE, (c) BLG-MWCNTs-GNPs/GCE recorded in 0.1 M KCl aqueous containing 10 mM $[Fe(CN)^6]^{3-}$. Scan rate: 50 mV s^{-1}.

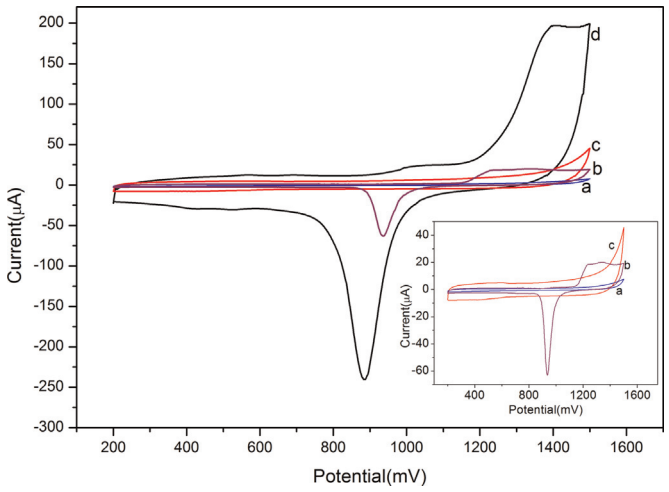

Fig. 3. Cyclic voltammograms of (a) unmodified GCE, (b) GNPs/GCE, (c) BLG–MWCNTs/GCE and (d) BLG-MWCNTs-GNPs/GCE in 0.5 M H_2SO_4 at the scan rate of 50 mV s^{-1}. Inset shows amplified CVs for a, b, and c.

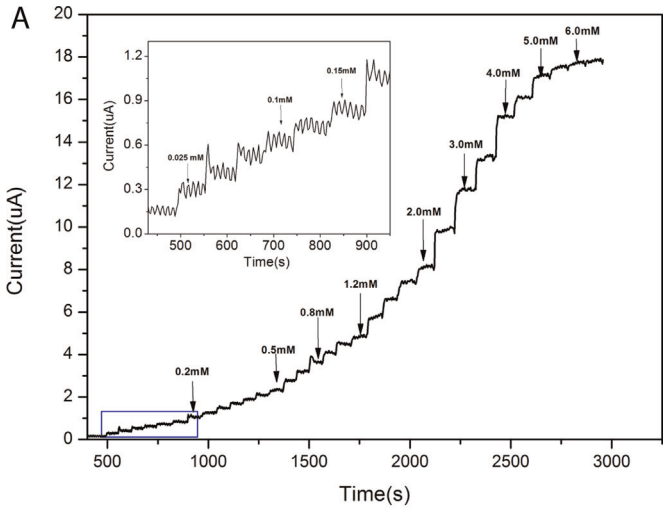

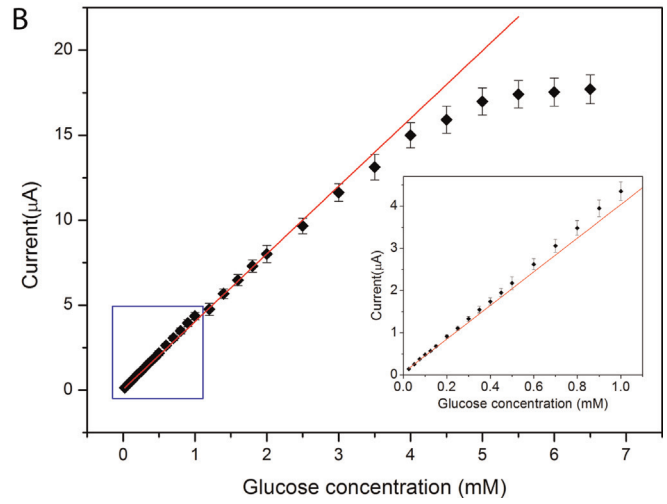

Fig. 4. (A) Amperometric response of GOD/BSA/BLG-MWCNTs-GNPs/GCE upon successive additions of glucose in 0.1 M PBS (pH 7.0) at 600 mV. Inset: amplification of the i–t curve at the lower concentration region. (B) The calibration curve. Inset: amplification of the calibration graph at the lower concentration region. Error bars= ± standard deviation and n=5.

the redox peaks of GNPs proved the successful preparation of BLG-MWCNTs-GNPs again.

Satisfactory electrocatalytic activity of BLG-MWCNTs-GNPs indicated that the nanocomposite can be used in various electrochemical detections. Substances that have electron transfer in solution can be detected directly, such as H_2O_2, dopamine. Furthermore, because of the facile fabrication method, nontoxicity and biocompatibility of BLG-MWCNTs-GNPs, the nanocomposite provided a perfect platform for various fields. DNA, various cell lines, drugs and other biomolecules can be attached to the surface of BLG-MWCNTs-GNPs, and then these composites can be applied to DNA detection, biosensing, and therapies in vitro or vivo. Owing to the biocompatibility of BLG-MWCNTs-GNPs, the bio-enzyme can keep its activity on the nanocomposite for a long time. In our works, we employed GOD as a model enzyme to evaluate the electrocatalytic ability and biocompatibility of the BLG-MWCNTs-GNPs.

3.3. *Electrochemical performance of GOD/BSA/BLG-MWCNTs-GNPs/GCE towards glucose*

The amount of GNPs loading on BLG-MWCNTs may directly affect the electrocatalytic activity of GOD/BSA/BLG-MWCNTs-GNPs/GCE. Therefore, we investigated the effect of electrodeposition time. As shown in Fig. S2, the current response to 3 mM glucose increased with the increasing electrodeposition time from 120 s to 360 s and reached the maximum, followed by current decrease. This may be associated with the fact that the size of GNPs increased and the electrochemical active area decreased, which blocks the electron transfer. Therefore, we chose the 360 s as the optimum electrodeposition time. The CVs of GOD/BSA/BLG-MWCNTs-GNPs/GCE in 10 mM glucose solution and PBS at pH 7.0 were recorded (Fig. S3). We can see an obvious anodic peak which can be ascribed to H_2O_2 produced by the GOD-catalyzed oxidation of glucose in the presence of oxygen (Guiseppi-Elie et al., 2002). Moreover, the maximal peak current occurred at around +600 mV, which was adopted as the working potential.

The typical amperometric responses to glucose of GOD/BSA/BLG-MWCNTs-GNPs/GCE are shown in Fig. 4A. The current response increased gradually with the increasing glucose concentration within limit. After that, because of the saturation of GOD and the reducing of oxygen content, the growth rate decreased and then reached the maximum which according with the typical kinetics of enzyme catalyzed reaction. Furthermore, we can find

Table 1
Comparison of selected electrochemical sensors for glucose detection.

Electrode material	LOD (μM)	Liner range (mM)	Sensitivity (μA mM^{-1})	Reference
Cobalt phthalocyanine	–	0.2–5	1.12	Crouch et al. (2005)
Chitosan	100	0.6–2.8	0.233	Zhao et al. (2008)
ZnO nanorod	10	0.01–0.25/0.3–0.7	–	Yang et al. (2010)
Nafion-Ag-Pdop[a]@CNT	17	0.05–1.1	3.1	Y. Wang et al. (2011)
GNPs-SAM[b]-PNT[c]	73.1	0.5–2.4	0.3	Park et al. (2012)
Pt-OMC[d]	50	0.05–3.7	0.38	Jiang et al. (2011)
TiO_2 nanotube	3.8	0.05–0.65	–	Wang et al. (2014)
BLG-MWCNTs-GNPs	1.1	0.025–5.5	3.98	This work

[a] Polydopamine.
[b] Binary self-assembled monolayer.
[c] Bio-inspired peptide nanotube.
[d] Ordered mesoporous carbon.

the current response reached 95% steady-state current within 7 s. After five independent repetitive experiments, the calibration curve was fitted and shown in Fig. 4B, which gave a linear response to glucose over the centration from 0.025 to 5.5 mM with a correlation coefficient of 0.996 (RSD varied from 3.3% to 4.8%, $n=5$). The sensitivity was calculated to be 3.98 μA mM^{-1} (56.3 μA mM^{-1} cm^{-2}). The limit of detection (LOD) was found to be 1.1 μM at the signal-to-noise ratio of 3. The Michaelis–Menten constant (K_m) of the GOD/BSA/BLG-MWCNTs-GNPs/GCE can be calculated based on the conventional Lineweaver–Burk equation (Kamin and Wilson, 1980). The K_m value was calculated to be 2.47 mM which was much lower than that in the literatures reported before (Peng et al., 2011; Zhou et al., 2013). The low K_m can be attributed to the fact that BLG-MWCNTs-GNPs can adsorbed much GOD and held the enzymatic activity more easily because its large specific surface area, fast electron transfer rate and biocompability. In Table 1, we compared the performance characteristics of the present glucose sensor with the sensors previously reported by others. As can be seen, the proposed GOD/BSA/BLG-MWCNTs-GNPs/GCE showed better performances than other glucose sensors in the respects of LOD, linear range and sensitivity.

3.4. *Selectivity, stability and reproducibility of the modified electrode*

We have studied possible interference from ascorbic acid, uric acid and acetaminophen to evaluate the selectivity of the GOD/BSA/BLG-MWCNTs-GNPs/GCE. The current responses to 0.15 mM ascorbic acid and 0.15 mM acetaminophen were 0.56 μA and 0.54 μA, respectively. The current response to 0.5 mM uric acid was negligible. The current responses of the interference were minor compared to the high sensitivity of the modified electrode. In addition, the modified electrode had superior stability. When not in use, the electrode was stored at 4 °C in PBS (pH 7.0) and it can remain 79.6% of the current response after one month. The reproducibility was investigated from the current response to 3 mM glucose at +600 mV using five different BLG-MWCNTs-GNPs/GCEs prepared by the same way (as shown in Fig. S4). The relative standard deviation (RSD) was 4.6%, which reveals the glucose sensor has excellent reproducibility. Long-term stability and excellent reproducibility of the modified electrode demonstrated that the BSA/BLG-MWCNTs-GNPs provided a biocompatible microenvironment to maintain the activity of the enzyme and the construction process was very mild.

4. Conclusions

In summary, we fabricated the BLG–MWCNTs-GNPs nanocomposite by a facile way for the first time. A novel glucose biosensor was developed based on the BLG–MWCNTs-GNPs film which displayed low detection limit, high sensitivity and fast response time for glucose detection. We believe that the excellent electrocatalytic activity, biocompatibility and stability of BLG-MWCNTs-GNPs would provide a new platform for biosensors, immunoassays, DNA detection and drug delivery. Furthermore, the advantages of ease-of-synthesis and low cost would potentially lead the protein-functionalized MWCNTs and their nanocomposites to be more popular in the research of biochemical sensing. Therefore, we are quite optimistic about the further applications and development of this research.

Acknowledgments

The financial supports from National Natural Science Foundation of China (Grant nos. 81127001 and 81273993) are acknowledged.

Appendix A. Supplementary material

Supplementary data associated with this article can be found in the online version at http://dx.doi.org/10.1016/j.bios.2014.06.030.

References

Abdelhalim, A., Abdellah, A., Scarpa, G., Lugli, P., 2014. Nanotechnology 25, 5.
Atthipalli, G., Tang, Y., Star, A., Gray, J.L., 2011. Thin Solid Films 520 (5), 1651–1655.
Belgorodsky, B., Fadeev, L., Kolsenik, J., Gozin, M., 2007. Bioconj. Chem. 18 (4), 1095–1100.
Burke, L.D., Buckley, D.T., Morrissey, J.A., 1994. Analyst 119 (5), 841–845.
Chen, J., Hamon, M.A., Hu, H., Chen, Y.S., Rao, A.M., Eklund, P.C., Haddon, R.C., 1998. Science 282 (5386), 95–98.
Crouch, E., Cowell, D.C., Hoskins, S., Pittson, R.W., Hart, J.P., 2005. Anal. Biochem. 347 (1), 17–23.
Elouarzaki, K., Haddad, R., Holzinger, M., Le Goff, A., Thery, J., Cosnier, S., 2014. J. Power Sources 255, 24–28.
Fang, Y.X., Zhang, D., Qin, X., Miao, Z.Y., Takahashi, S., Anzai, J., Chen, Q., 2012. Electrochim. Acta 70, 266–271.
Feng, X.M., Hu, J.Q., Chen, X.H., Xie, J.S., Liu, Y.Y., 2009. J. Phys. D: Appl. Phys. 42, 4.
Fragneto, G., Su, T.J., Lu, J.R., Thomas, R.K., Rennie, A.R., 2000. Phys. Chem. Chem. Phys. 2 (22), 5214–5221.
Gao, X., Wei, W., Yang, L., Guo, M., 2006. Electroanalysis 18 (5), 485–492.
Geyik, C., Evran, S., Timur, S., Telefoncu, A., 2014. Biotechnol. Progr. 30 (1), 224–232.
Guiseppi-Elie, A., Lei, C.H., Baughman, R.H., 2002. Nanotechnology 13 (5), 559–564.
Haghighi, B., Bozorgzadeh, S., Gorton, L., 2011. Sens. Actuators B: Chem. 155 (2), 577–583.
Jiang, X., Wu, Y., Mao, X., Cui, X., Zhu, L., 2011. Sens. Actuators B: Chem. 153 (1), 158–163.
Kamin, R.A., Wilson, G.S., 1980. Anal. Chem. 52 (8), 1198–1205.
Liang, L., Tajmir-Riahi, H.A., Subirade, M., 2008. Biomacromolecules 9 (1), 50–56.
Majeed, S., Filiz, V., Shishatskiy, S., Wind, J., Abetz, C., Abetz, V., 2012. Nanoscale Res. Lett. 7, 1–11.
Mensi, A., Choiset, Y., Rabesona, H., Haertle, T., Borel, P., Chobert, J.M., 2013. J. Agric. Food Chem. 61 (17), 4114–4119.

Munoz, E., Sreelatha, A., Garriga, R., Baughman, R.H., Goux, W.J., 2013. J. Phys. Chem. B 117 (25), 7593–7604.
Park, B.W., Zheng, R., Ko, K.A., Cameron, B.D., Yoon, D.Y., Kim, D.S., 2012. Biosens. Bioelectron. 38 (1), 295–301.
Peng, Y., Wei, C.W., Liu, Y.N., Li, J., 2011. Analyst 136 (19), 4003–4007.
Sahihi, M., Ghayeb, Y., Bordbar, A.K., 2013. Chem. Biochem. Eng. Q 27 (4), 417–422.
Sakai, K., Sakurai, K., Sakai, M., Hoshino, M., Goto, Y., 2000. Protein Sci. 9 (9), 1719–1729.
Shao, L., Mu, C.Z., Du, H.P., Czech, Z., Du, H.C., Bai, Y.P., 2011. Appl. Surf. Sci. 258 (5), 1682–1688.
Voge, C.M., Johns, J., Raghavan, M., Morris, M.D., Stegemann, J.P., 2013. J. Biomed. Mater. Res. A 101A (1), 231–238.
Wang, S.Y., Yu, D.S., Dai, L.M., 2011. J. Am. Chem. Soc. 133 (14), 5182–5185.
Wang, W., Xie, Y.B., Wang, Y., Du, H.X., Xia, C., Tian, F., 2014. Microchim. Acta 181 (3–4), 381–387.
Wang, X.S., Wang, H.C., Huang, Y.J., Zhao, Z.X., Qin, X., Wang, Y.Y., Miao, Z.Y., Chen, Q. A., Qiao, M.Q., 2010. Biosens. Bioelectron. 26 (3), 1104–1108.
Wang, Y., Liu, L., Li, M., Xu, S., Gao, F., 2011. Biosens. Bioelectron. 30 (1), 107–111.
Yang, Z., Ye, Z., Zhao, B., Zong, X., Wang, P., 2010. Physica E: Low-dimensional Systems Nanostruct. 42 (6), 1830–1833.
Zhang, J., Zhu, Z.X., Zhu, J.L., Li, K.C., Hua, S.C., 2014. Int. J. Electrochem. Soc. 9 (3), 1264–1272.
Zhao, C., Meng, Y., Shao, C., Wan, L., Jiao, K., 2008. Electroanalysis 20 (5), 520–526.
Zhou, Y., Wang, L., Ye, Z.Z., Zhao, M.G., Cai, H., Huang, J.Y., 2013. Appl. Surf. Sci. 285, 344–349.